Plasma-Assisted Nanoscale Protein Patterning on Si Substrates via Colloidal Lithography

ARTICLE *in* THE JOURNAL OF PHYSICAL CHEMISTRY A · NOVEMBER 2013

Impact Factor: 2.69 · DOI: 10.1021/jp407810x · Source: PubMed

THE JOURNAL OF PHYSICAL CHEMISTRY A

Article

pubs.acs.org/JPCA

Plasma-Assisted Nanoscale Protein Patterning on Si Substrates via Colloidal Lithography

A. Malainou,[†] K. Tsougeni,[†] K. Ellinas,[†] P. S. Petrou,[‡] V. Constantoudis,[†] E. Sarantopoulou,[§] K. Awsiuk,[∥] A. Bernasik,[∥] A. Budkowski,[∥] A. Markou,[⊥] I. Panagiotopoulos,[⊥] S. E. Kakabakos,[‡] E. Gogolides,[†] and A. Tserepi*,[†]

[†]Department of Microelectronics, Institute of Advanced Materials, Physicochemical Process, Nanotechnology & Microsystems, NCSR "Demokritos", 15310 Aghia Paraskevi, Attiki, Greece

[‡]Immunoassay/Immunosensors Laboratory, Institute of Nuclear and Radiological Sciences, Energy, Technology and Safety, NCSR "Demokritos", 15310 Aghia Paraskevi, Attiki, Greece

[§]National Hellenic Research Foundation, Theoretical and Physical Chemistry Institute, 11635, Athens, Greece

[∥]M. Smoluchowski Institute of Physics, Jagiellonian University, Reymonta 4, 30-059 Kraków, Poland

[⊥]Department of Materials Science and Engineering, University of Ioannina, Greece

Supporting Information

ABSTRACT: Selective immobilization of proteins in well-defined patterns on substrates has recently attracted considerable attention as an enabling technology for applications ranging from biosensors and BioMEMS to tissue engineering. In this work, a method is reported for low-cost, large scale and high throughput, selective immobilization of proteins on nanopatterned Si, based on colloidal lithography and plasma processing to define the areas (<300 nm) where proteins are selectively immobilized. A close-packed monolayer of PS microparticles is deposited on oxidized Si and, either after microparticle size reduction or alternatively after metal deposition through the PS close-packed monolayer, is used as etching mask to define SiO_2 nanoislands (on Si). C_4F_8 plasma was used to selectively etch and modify the SiO_2 nanoislands while depositing a fluorocarbon layer on the Si surface. The plasma-treated surfaces were chemically characterized in terms of functional group identification through XPS analysis and reaction with specific molecules. Highly selective protein immobilization mainly through physical adsorption on SiO_2 nanoislands and not on surrounding Si was observed after C_4F_8 plasma-induced chemical modification of the substrate. The thickness of the immobilized protein monolayer was estimated by means of AFM image analysis. The method reported herein constitutes a cost-efficient route toward rapid, large surface, and high-density patterning of biomolecules on solid supports that can be easily applied in BioMEMS or microanalytical systems.

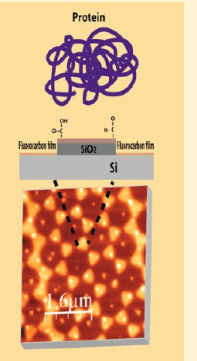

1. INTRODUCTION

The potential of proteins to be immobilized on micro- or nanofabricated devices is steadily gaining importance for application in biosensors, BioMEMS, protein arrays, as well as tissue engineering.[1−7] Protein patterning involves immobilization of biomolecules in particular areas on solid surfaces while preventing protein attachment on the rest of the surface.[8,9] The desired feature size depends on the application, and the advancement of technology from micro- to nanofabrication has favored protein patterning shift from the microscale to the nanoscale for applications ranging from biosensors and protein arrays to basic studies of single protein interactions and cell attachment.[10−14]

To create protein patterns, photolithography-based methods have been extensively used.[8] However, for features smaller than 1 μm, photolithography using contact or proximity printing is reaching its limits and becomes non cost-efficient. On the other hand, dip-pen lithography (using AFM tips) and e-beam lithography that can successfully achieve nanoscale patterning involve complex and high-cost apparati, are serial processes and, as such, lack scalability.[8,15]

A versatile, easy, fast, flexible, and low-cost lithographic method to reach successfully the nanometer scale is colloidal lithography. Its capability for high-resolution patterning renders it appropriate for nanoscale protein patterning in emerging biomedical applications.[16,17]

Colloidal lithography is based on the close-packed self-assembly of colloidal microparticles over large surface areas. This method has been extensively used as a patterning technique,[10,11,14,16,18−21] with the colloidal particles acting as masks in metal/polymer deposition and/or plasma etching.[15,16,22−26] Moreover, colloidal microparticles are used for the enhancement of surface nanotopography.[16,27,17]

In this work, we report a novel protein nanopatterning method using colloidal lithography[11,16] and plasma-based[12,28,29] chemical modification of SiO_2/Si substrates in C_4F_8[27] that

Special Issue: Terry A. Miller Festschrift

Received: August 5, 2013
Revised: October 31, 2013

   dx.doi.org/10.1021/jp407810x | J. Phys. Chem. A XXXX, XXX, XXX−XXX

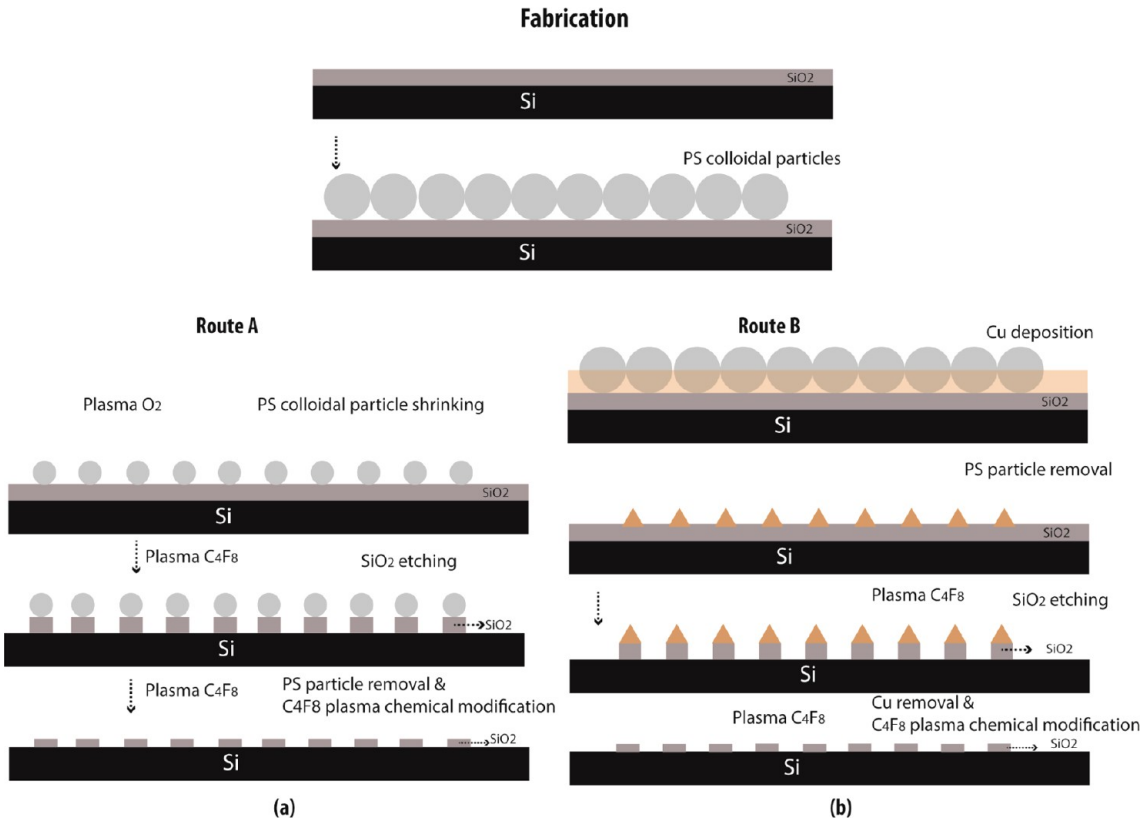

Figure 1. Schematic of the two processes for fabrication of SiO_2 nanoislands on Si substrates.

enables selective immobilization of proteins only on the plasma-modified SiO_2 nanoislands and not on the plasma-modified Si surface. The greatest advantage of our method is the simplicity of the procedure employed for selective chemical modification of the surface, i.e., short plasma treatment, as compared to functionalization protocols based on wet chemistries.[7,13,15,16,23,24,26,30] We demonstrate SiO_2 nanoislands patterned on a Si substrate, using a two-dimensional (2D) closed-packed monolayer of colloidal particles after size reduction or alternatively deposited metal islands between the particles, as an etching mask for defining the SiO_2 nanoislands. Following an optimized plasma treatment, selective immobilization of proteins is achieved on the SiO_2 nanoislands with respect to Si.[28] The thickness of the selectively immobilized protein layer on SiO_2 is estimated by means of atomic force microscopy (AFM) and Matlab-based software for image analysis. Finally, to elucidate the chemical composition of our plasma-modified substrates, we combined XPS spectroscopy with identification of the major functional groups after reaction with specific biomolecules. The latter were selected to form covalent bonds with carboxyl and/or carbonyl groups. The confirmed presence of such functional groups on SiO_2 surfaces, as a result of selective plasma modification of our substrates, suggests the possibility of covalent protein binding on such surfaces apart from physical adsorption.

2. EXPERIMENTAL SECTION

2.1. Materials. Typical 3 in. silicon wafers with thermally grown oxides (with a thickness of 60 nm) were used as substrates after cleaning in piranha solution (H_2SO_4/H_2O_2 1:1) to remove any possible contamination. (***Caution!*** Piranha solution is aggressive and explosive. Never mix piranha waste with solvents. Check the safety precautions before using it.) A suspension of 0.92 μm polystyrene (PS) particles in water were purchased from Mikropartikel Gmbh. Triton X-100 was purchased from Sigma Aldrich. Plasma treatment was performed using O_2 and c-C_4F_8 gas provided by Air Liquide Hellas.

Bovine serum albumin (BSA, Cohn fraction V, RIA grade), D-biotin and biotinamidohexanoic acid hydrazide were also purchased from Sigma Chemical Co. (St. Louis, MO, USA). Amine-PEG_3-biotin, EDC (1-ethyl-3-[3-(dimethylamino)-propyl]carbodiimide hydrochloride), and sulfo-NHS (*N*-hydroxysulfosuccinimide) were purchased from Thermo Fisher Scientific Inc. (Rockford, IL, USA). Streptavidin labeled with AlexaFluor 546 (AF546) was purchased from Molecular Probes, Inc. (Eugene, OR, USA).

2.2. Methods. *2.2.1. Colloidal Lithography.* Spin coating was used for the deposition of colloidal particles on oxidized Si substrates. A PS bead solution was prepared by mixing equal volumes of particle suspension in water with a 1:400 (v/v) Triton X-100/methanol solution. Triton-X is used to reduce the surface tension of the particle aqueous solution and thus increase the adhesion of the particles with the piranha-cleaned substrates. The coating process consisted of two steps: (a) a dispersion step at 200−300 rpm/min for approximately 30 s and (b) a second spinning step at 1000 rpm/min for 10−15 s, to remove the excess bead solution, as described in detail in our previous work.[31]

2.2.2. Plasma Processing. Plasma processing of the substrates took place in a high-density plasma reactor (Helicon plasma reactor, Micromachining Etching Tool, MET, from Alcatel).

dx.doi.org/10.1021/jp407810x | J. Phys. Chem. A XXXX, XXX, XXX−XXX

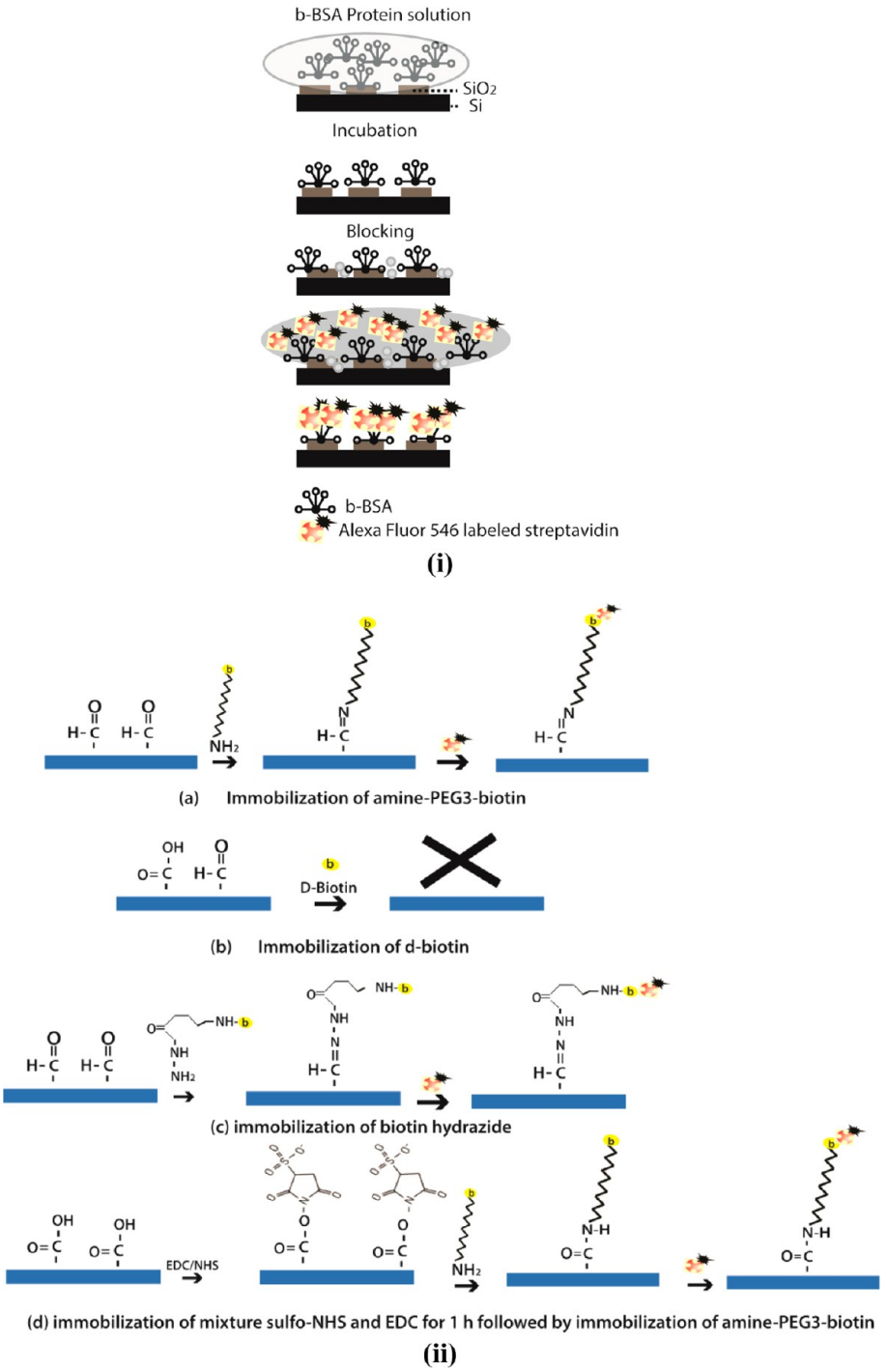

Figure 2. (i) Process flow for selective b-BSA protein immobilization on selectively modified patterned substrates. (ii) Processes of covalent attachment and detection of biotin derivatives on Si and SiO_2 surfaces.

For PS particle size reduction, isotropic O_2 plasma was used (gas pressure, 0.75 Pa; electrode temperature, 15 °C; O_2 flow rate, 100 sccm; plasma source power, 1900 W; bias voltage, 0 V).

For SiO_2 etching, between the PS microparticles or the copper nanoislands, as well as the selective chemical modification of the SiO_2 with respect to Si areas, a c-C_4F_8 plasma was used at the following conditions: gas pressure of 0.26 Pa, electrode temperature of 0 °C, C_4F_8 flow of 25 sccm, plasma source power of 800 W, electrode bias at −160 V.

2.2.3. Copper Deposition. Cu films with a total thickness of 28 nm were deposited by magnetron sputtering at room temperature using a MANTIS deposition system from a Cu (2 in. disk) target. Prior to the deposition, the chamber was evacuated to a base pressure of 7×10^{-7} Torr and the process gas (Ar 5N) pressure was 2.5 mTorr. A deposition rate of 5.1 ± 0.1 nm/min was achieved by applying 60W RF.

2.2.4. Substrate Patterning. After PS particle spin-coating on SiO_2, a closely packed particle assembly is produced. Two different routes are then employed to create ordered arrays of SiO_2 nanoislands (Figure 1).

dx.doi.org/10.1021/jp407810x | J. Phys. Chem. A XXXX, XXX, XXX−XXX

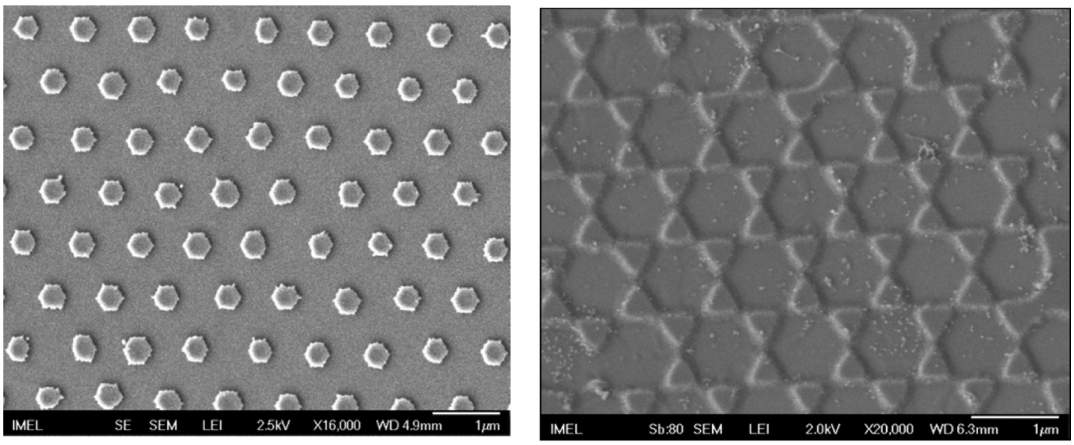

Figure 3. SEM images of our patterned SiO_2/Si substrates. SiO_2 nanoislands of (a) circular shape, 300 nm in diameter, fabricated following route A, and (b) triangular shape, with a side of 300 nm, fabricated following route B, are depicted.

According to the first route (route A), the substrate patterning process consists of a two-step plasma etching. First, an isotropic etching step in O_2 plasma takes place in order to shrink the particles followed by an anisotropic plasma treatment step in C_4F_8 to completely remove the 60 nm thick SiO_2 layer from the areas between the particles. This allows the fabrication of SiO_2 nanoislands of controlled diameter depending on the etching time and the applied bias voltage. Subsequently, the PS particles are removed from the top of the SiO_2 nanoislands using a strong adhesive tape (Figure 1a).

The second route (route B) involves copper deposition in the interstices between the particles right after spin-coating of colloidal particle solution on SiO_2/Si substrates (Figure 1b). PS particles are removed and the copper remained islands are utilized as etch mask during an anisotropic plasma etching step in C_4F_8, which completely removes the 60 nm thick SiO_2 layer from the areas between the copper islands. After that step, copper is removed and the SiO_2 nanoislands are revealed on Si. For copper removal, a commercial PCB copper etchant, sodium persulfate, was used (100 gr of powder diluted in 500 mL water at 50 °C).

Finally, in both routes, an optimized treatment step in c-C_4F_8 plasma is performed for selective chemical modification of the SiO_2 nanoislands with respect to Si areas.[28]

2.2.5. Protein Deposition. A model binding assay based on the biotin−streptavidin system was employed to demonstrate selective protein immobilization to freshly prepared, typically 1 day after C_4F_8 selective plasma treatment, nanopatterned surfaces. In particular, biotinylated bovine serum albumin (b-BSA) was immobilized onto the surface (without any additional chemical treatment of the surface) and was detected through reaction with fluorescently labeled streptavidin. Two-microlitter droplets of b-BSA solution (25 μg/mL) in 50 mM phosphate buffer, pH 7.4, were manually deposited onto the surface and incubated for 1 h at room temperature (RT) in a humidity chamber. After washing, the samples were immersed in a 10 g/L BSA solution in 50 mM phosphate buffer, pH 7.4 (blocking solution), for 1 h at RT, to cover the remaining free binding sites of the surface. The proteins immobilized onto the surface were detected through reaction with a 5 μg/mL solution of AF546-labeled streptavidin in blocking solution, for 30 min at RT. Subsequently, the surfaces were washed extensively with 50 mM phosphate buffer, pH 7.4, 0.05% Tween 20 (v/v), and distilled water and dried under N_2 stream. The protein immobilization and detection process is depicted schematically in Figure 2. The protein adsorption on the patterned substrates was confirmed by fluorescence images acquired through a confocal microscope.

2.2.6. Covalent Binding of Biotin Derivatives. All processes followed for covalent binding of activated biotin derivatives onto the patterned and plasma-assisted functionalized surface as well as their detection are schematically depicted in Figure 2(ii). To identify the presence of carbonyl groups on the surfaces, the direct immobilization of (a) amine-PEG_3-biotin, (b) biotinamidohexanoic acid hydrazide, and (c) D-biotin was investigated. All three reagents were diluted at a concentration of 25 mM in 0.1 M $NaHCO_3$ solution, pH 8.5, and 10 μL droplets of each solution were deposited onto the surfaces. Incubation for 2 h at RT in a humidity chamber was implemented.

For the detection of carboxyl groups onto the surfaces, a two-step approach was followed: (1) activation of carboxyl groups by a EDC/NHS mixture (10 mM EDC and 5 mM sulfo-NHS in 0.1 M MES buffer, pH 5) for 1 h at RT. (2) Coupling of amine-PEG_3-biotin from a 25 mM solution in 0.1 M $NaHCO_3$ solution, pH 8.5, for 2 h at RT.

Then all samples were washed with 0.1 M $NaHCO_3$ solution, pH 8.5, and immersed in a 10 g/L BSA solution in 50 mM phosphate buffer, pH 7.4 (blocking solution), for 1 h at RT to cover the remaining free binding sites of the surface. After that, the surfaces were washed three times with 50 mM phosphate buffer, pH 7.4. The immobilized biotin derivatives on the surface were detected through reaction with a 2.5 μg/mL AF546-labeled streptavidin in blocking solution, for 30 min at RT. Subsequently, the surfaces were washed extensively five times with 50 mM phosphate buffer, pH 7.4, and distilled water and dried under a stream of N_2. Fluorescence images were acquired with an Axioskop 2 Plus epifluorescence microscope (Carl Zeiss) equipped with a Sony Cyber-Shot 8-bit digital camera and processed with ImagePro Plus software (Media Cybernetics, Inc.).

2.2.7. Surface Characterization. A JEOL JSM-7401F FEG SEM was used for observation of the surfaces after colloidal lithography and plasma treatment. Also, a confocal microscope from Leica Microsystems (TCS SP5) was used for observation of the surfaces after protein immobilization and reaction with

dx.doi.org/10.1021/jp407810x | J. Phys. Chem. A XXXX, XXX, XXX−XXX

fluorescently labeled binding molecules, to demonstrate selective protein adsorption on the SiO_2 nanoislands.

The surface topography was characterized by an atomic force microscope (AFM, Veeco diInnova) in the tapping mode. The scanning rate was 1 kHz, and the scanned area $4 \times 4\ \mu m^2$ with 512×512 pixel resolution. After a second-order polynomial plane correction, the root-mean-square (rms) surface roughness was calculated from the software of the instrument.

The chemical composition of the surfaces prior to and after plasma treatment was investigated by XPS analysis. The spectra were recorded on a PHI 5000 VersaProbe II (ULVAC-PHI, Chigasaki, Japan) system using a microfocused (100 μm, 25 W) Al Kα X-ray beam with a photoelectron takeoff angle of 45°. A dual-beam charge neutralizer was used to compensate the charge-up effect. High-resolution spectra were collected with analyzer pass energy of 23.5 eV. The operating pressure in the analytical chamber was less than 5×10^{-7} Pa. All XPS peaks were referenced to the neutral (C−C) carbon C1s peak, at a binding energy of 284.8 eV. Spectral backgrounds were subtracted using the Shirley method.

3. RESULTS AND DISCUSSION

3.1. Patterned Substrates. Following the above-described method of surface nanopatterning, Scanning electron microscopy (SEM) was performed, to evaluate our nanopatterned substrates before protein deposition. The images in Figure 3a,b show the formation of SiO_2 nanoislands, of circular or triangular shape (depending on the fabrication route) with a maximum dimension of 300 nm. It should be pointed out that although the final SiO_2 feature size obtained through PS microparticle shrinking (route A) can be as low as possible depending on the etching time of the shrinking step, high particle size variability was observed at long etching times; therefore, shorter etching durations were preferred, i.e., 130 s etching, leading to microparticle shrinking to about one-third of their initial size (Figure 3a). The size of the triangular-like SiO_2 islands shown in Figure 3b is defined by the areas left between the 2D closed-packed PS microparticle arrays, and each equilateral side is approximately 300 nm.

3.2. Chemical Analysis of Si and SiO_2 Surfaces. After nanopatterning, our substrates undergo a short (15 s) C_4F_8 plasma step, optimized such that although a fluorocarbon layer is deposited on Si areas, SiO_2 areas remain hydrophilic (water contact angle of 60°). We have shown that on micropatterned substrates[28] this step leads to a distinct chemical modification of SiO_2 with respect to Si areas, which in turn leads to selective immobilization of proteins on SiO_2 areas mainly by physical adsorption, with no other functionalization being necessary. The overall atomic composition of the Si and SiO_2 surfaces before and after plasma treatment is shown in Table 1. As expected, the overall C atomic concentration in both plasma-modified substrates was increased, in Si from 8.9% to 27% and in SiO_2 from 3.8% to 10.5%. More importantly, the modified Si surfaces show a significant increase of the F atomic concentration from ∼0% to ∼25.2% after 15 s treatment. On the other hand, the F atomic concentration of the modified SiO_2 surfaces increased less (from ∼0% to ∼7.0%) compared to Si surfaces.

Table 1. Composition (Atomic Element Concentration) of Si and SiO_2 Surfaces before and after Plasma Modification

At (%)	Si untreated	Si C_4F_8-treated	SiO_2 untreated	SiO_2 C_4F_8-treated
C	8.9	26.7	3.8	10.5
Si	49.8	28.9	30.3	26.2
O	41.4	17.8	65.9	55.7
F	0.0	25.2	0.0	7.0
N	0.0	1.4	0.0	0.6

To investigate the plasma-induced chemical modification of our substrates, further XPS analysis was performed before and after plasma treatment, followed by curve fitting analysis for both the C1s and F1s spectra. The contribution of all components and curve fitting data of the C1s spectra for Si and SiO_2 before and after 15 s C_4F_8 plasma treatment are shown in Table 2. The C1s spectra of untreated SiO_2 and Si samples are characterized basically by the presence of C−C and C−O moieties, typical for native Si and SiO_2 surfaces. Additional components are introduced in both Si and SiO_2 samples from the plasma modification step, as it is suggested by the XPS data. Analysis revealed additional contributions from $-[CF_2]_n-$ (287.6 eV), COOH or CF (289 eV), CF_2 (291.3 eV), and CF_3 (293.6 eV) groups, whereas the contribution of the C−O or CF_x-CH_2 (286.4 eV) component is greatly enhanced. This result shows that a Teflon-like film in $-(CF_n)-$ form is deposited selectively on Si substrate after C_4F_8 plasma, confirming our previous results.[28] In addition, careful examination of Table 2 shows that peaks like (C−O) CF_x-CH_2 and COOH or CF appeared to a higher proportion after plasma modification on SiO_2 compared to Si. The presence of COOH and C═O is proved below through reaction with appropriately functionalized biotin derivatives.

3.3. Detection of Specific Functional Groups for Covalent Binding. To determine the presence of carboxyl and/or carbonyl groups (that could be used for covalent immobilization of biomolecules) on the plasma-modified SiO_2 and Si surfaces compared to untreated ones, we used biotin derivatives that are designed to form covalent bonds with common functional groups like carboxyl (−COOH) or carbonyl (C═O). The reagents used were (1) amine-PEG_3-Biotin, (2) D-biotin, (3) biotinamidohexanoic acid hydrazide, and (4) a mixture of sulfo-NHS and EDC followed by amine-PEG_3-biotin (see Experimental Section). C_4F_8 plasma treatment forms C—C, C═O and $CF_x-{}^*CH_2$, $(CF_2)_n$, COOH, and CF groups onto plasma-modified SiO_2 and Si, as revealed with XPS (see previous section), through which the above biotin derivatives are covalently attached to the surfaces. More specifically, the $-NH_2$ group of the amine-PEG_3-biotin and the hydrazide group from biotinamidohexanoic acid hydrazide covalently links to carbonyl groups from the plasma-treated substrate. Please note that hydrazides react more efficiently to carbonyl groups, thus confirming the presence of these specific groups onto the treated surfaces. Also the mixture sulfo-NHS and EDC activates the carboxyl groups from the modified substrate forming an amine-reactive O-acylisourea intermediate. This intermediate reacts then readily with the $-NH_2$ group of the amine-PEG_3-biotin, yielding a stable amide bond. D-biotin was used as a control biomolecule to exclude binding of the derivatives from sites other than their specific functional groups, because it has not a functional group that can covalently bind to carboxyl or carbonyl groups. In Figure 4a,b, the fluorescence intensities obtained from areas modified with the respective biotin derivatives are provided for both untreated and 15 s C_4F_8 plasma-treated Si and SiO_2 surfaces, after reaction with AF546-labeled streptavidin. The solid bars

dx.doi.org/10.1021/jp407810x | J. Phys. Chem. A XXXX, XXX, XXX−XXX

Table 2. Relative Percentage of Different Components in the C1s Peak for Si and SiO_2[a]

binding energy (eV)	284.8	286.4	287.7	289	291.3	293.5
moieties	(C−C) CH_2	(C−O) CF_x−CH_2	H replaced by F in $-[CH_2]_n-$	COOH and CF	$^{\wedge}CF_3$ | $-[CF-{}^{*}CF_2]_n-$ $^{\wedge}CF_3$	$^{*}CF_2$
Si untreated	76.5	19.6		4		
Si treated	37.9	18.6	13.4	11.6	5.0	13.5
SiO_2 untreated	85.9	14.6				
SiO_2 treated	42	19.6	6.2	16.3	3.9	12.1

[a]Typical binding energies are given at ±0.1 eV.

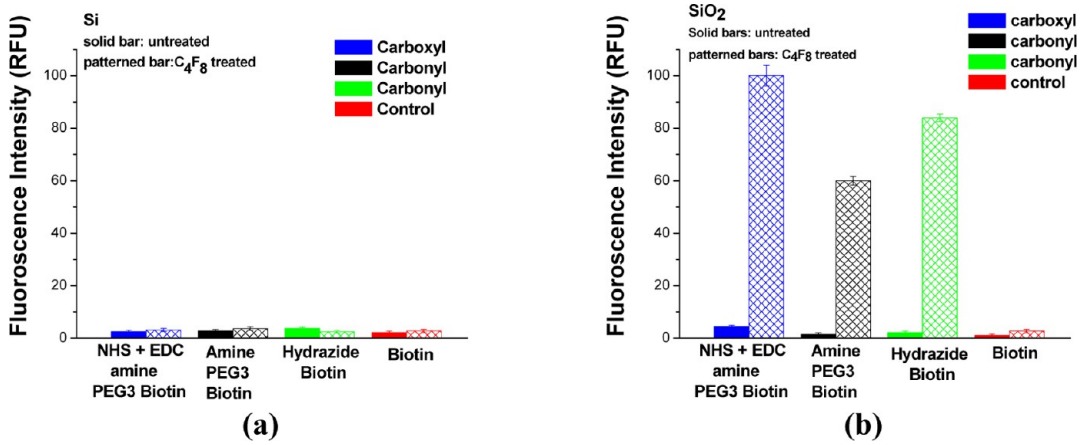

Figure 4. Fluorescence intensities obtained from areas modified with biotin derivatives: (1) amine-PEG_3-biotin (black bars), (2) sulfo-NHS followed by amine-PEG_3-biotin (blue bars), (3) D-biotin (red bars), and (4) biotin hydrazide (green bars) are provided after 2 h incubation and after reaction with AF546-labeled streptavidin on both untreated and 15 s C_4F_8 plasma-treated Si and SiO_2 surfaces.

represent the untreated substrates, whereas the patterned bars represent the treated substrates.

As shown in Figure 4a, both treated and untreated Si substrates exhibit fluorescence absolute values comparable to the untreated SiO_2 values. On the other hand, SiO_2 plasma-modified surfaces provided high fluorescence values, indicating reaction of carboxylic groups with NHS/EDC and/or amine biotin or of carbonyl groups with amine-PEG_3-biotin and biotin hydrazide. More specifically, the fluorescence values obtained by reacting the respective biotin derivative with surface carboxylic groups was 36-times higher than the value obtained by applying D-Biotin onto the same surface (control). Furthermore, the reaction of the surfaces with amine-PEG_3-biotin and hydrazide biotin provided 21- and 30-times higher fluorescence, respectively, compared with the control untreated surface.

These results suggest that C_4F_8 plasma treatment of SiO_2 leads to the formation of reactive and available carboxylic and carbonyl groups that can be used for covalent immobilization of biomolecules. Although the *potential* of such plasma-treated surfaces for covalent binding of biomolecules is indicated here, proteins are selectively immobilized on our plasma-modified SiO_2 surfaces mainly through physical adsorption. Nevertheless, covalent binding of proteins is also possible due to the existence of carboxyl and carbonyl groups on such surfaces, provided that functionalization of these groups by appropriate cross-linkers (e.g., EDC/NHS) will be first performed. We suspect that the presence of such groups selectively on the C_4F_8 plasma-treated SiO_2 surfaces (and not on Si surfaces) is a result of the reaction of plasma-deposited carbon with oxygen present on SiO_2 surface, as well as of aging when exposed to atmosphere after plasma treatment. However, we are convinced that our substrates are stable, because experiments performed several weeks after sample preparation did not exhibit any sign of deterioration of the selectivity between plasma-treated SiO_2 and Si surfaces.

3.4. Quantification of Protein Immobilization on SiO_2 Nanoislands. The selective binding of proteins onto C_4F_8 plasma-treated, nanopatterned substrates was first determined through fluorescence images taken after streptavidin specific binding to b-BSA by means of confocal microscopy. The latter provided a clear evidence that protein immobilization occurred selectively on SiO_2 nanoislands. However, due to the limited resolution of the method to depict the obtained nanoislands (300 nm), the reliable estimation of the achieved selectivity (i.e., spot to background fluorescence intensity ratio) was not possible by confocal microscopy. Thus, an alternative technique was selected on the basis of AFM imaging for the estimation of the thickness of the protein layer on the SiO_2 nanopatterns.[21,23,32] In fact, AFM imaging is widely used in the literature for protein thickness evaluation.[23] According to this approach, AFM images were taken before and after protein deposition and the height histograms of the measured surface topographies are plotted. They are expected to exhibit two peaks, the first one corresponding to the background (Si) surface, whereas the second peak corresponding to the nanoisland (SiO_2) surface. The distance between the peaks represents the nanoisland height in the image. After protein immobilization on the SiO_2 nanoislands, the second peak is expected to move to higher height values, and therefore the distance between the peaks is expected to increase. The amount of the increase in the peak difference gives an average

dx.doi.org/10.1021/jp407810x | J. Phys. Chem. A XXXX, XXX, XXX−XXX

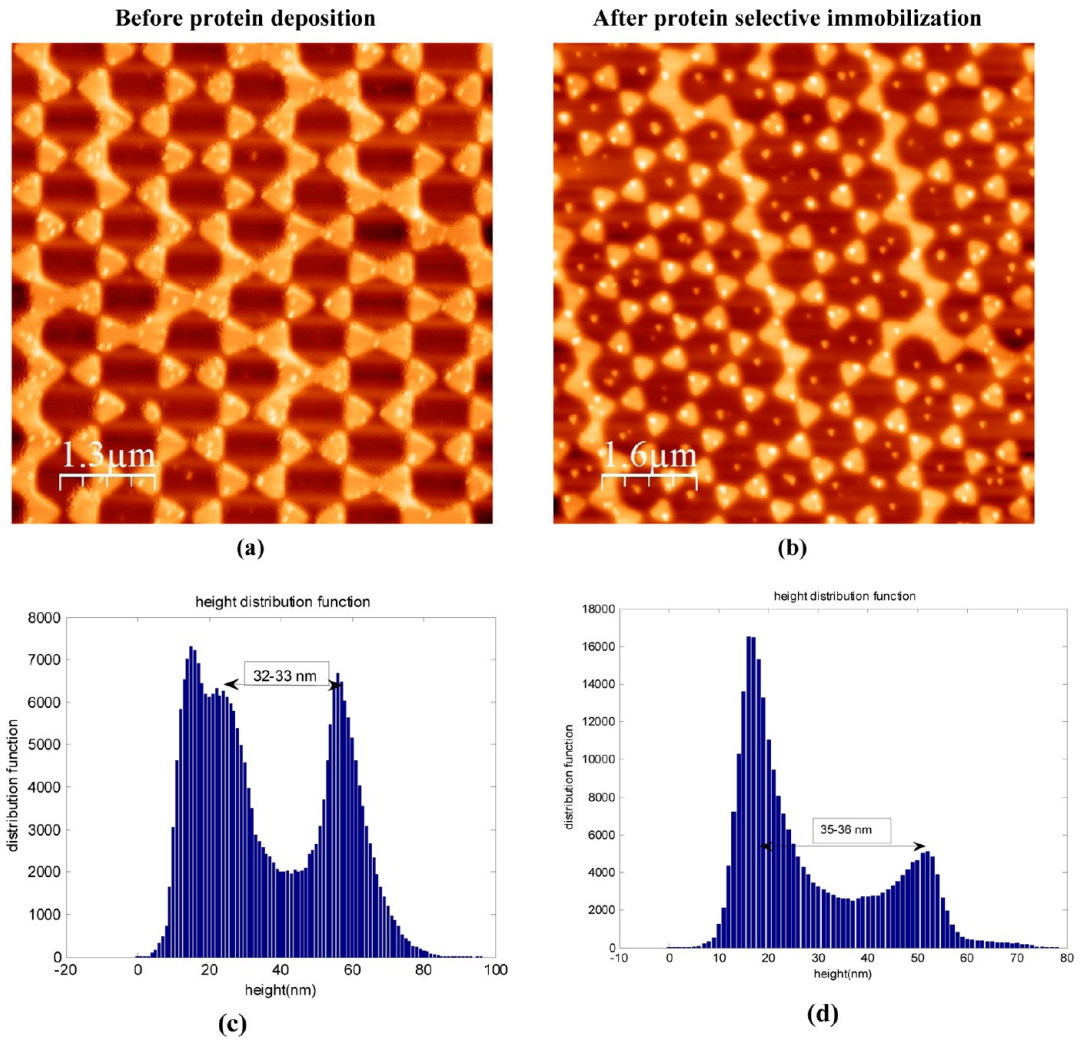

Figure 5. AFM images (a) before and (b) after b-BSA deposition, and (c), (d) corresponding surface height histograms after image analysis with "surfanalysis" (bin size 1).

estimation of the thickness of the deposited protein layer on SiO_2 nanoislands.

We have applied this method to our nanopatterned substrates and the results are shown in Figure 5, which depicts AFM images taken on the same sample consisting of posts with a diameter of 300 nm (route B), before (Figure 5a, scanning area: 5 × 5 μm^2) and after b-BSA deposition (Figure 5b, scanning area: 8 × 8 μm^2), and the respective height histograms (Figure 5c and Figure 5d) obtained after image analysis with the "surfanalysis" software developed in house.

In Figure 5c, the first peak which corresponds to the Si surface is composed of two peaks (Figure 5c), whereas this was not observed after protein immobilization (Figure 5d). This peak splitting is an artifact attributed to the color shading shown in Figure 5a (dark areas) for the Si surface, due to the "flying tip effect".[33] This artifact is quite usual and appears in AFM images when the tip scanning direction coincides with the post orientation. After it was realized that the first peak of the background surface height distribution was an artifact, the second peak was taken into account as the actual background peak. According to this, the histogram of Figure 5c indicates that the average height of the SiO_2 nanoislands is approximately 32−33 nm, also independently confirmed by means of SEM measurement of the SiO_2 nanoisland height (after C_4F_8 plasma treatment). Finally, it should be noted that the reason the "flying tip effect" was not observed in the images of Figure 5d (after protein immobilization) is due to the different AFM scanning orientation.

To increase the reliability of our measurements, we performed four AFM measurements, before and after protein immobilization, from which the SiO_2 height mean values were calculated and shown in Figure 6.

According to Figure 6, the mean value of the SiO_2 nanoisland height before protein deposition was 32 ± 0.5 nm, whereas the one corresponding to the nanoislands after protein immobilization was 35 ± 0.7 nm, suggesting a mean thickness of 3 ± 1 nm for the protein layer. This value is consistent with a BSA monolayer thickness (in dehydrated state) which is equal to 1.5−2 nm.[34,35] This finding further confirms the selective immobilization of proteins on our plasma-modified SiO_2 nanoislands. As discussed in the previous subsection (Detection of Specific Functional Groups for Covalent Binding), it is assumed that these proteins are mainly physisorbed on our plasma-modified SiO_2 surfaces, although covalent binding through available on the surface reactive groups cannot be completely excluded. Polymers subjected to ion-assisted plasma processes have been shown[29,36] to covalently immobilize biomolecules, due to reaction of biomolecules with surface

dx.doi.org/10.1021/jp407810x | J. Phys. Chem. A XXXX, XXX, XXX−XXX

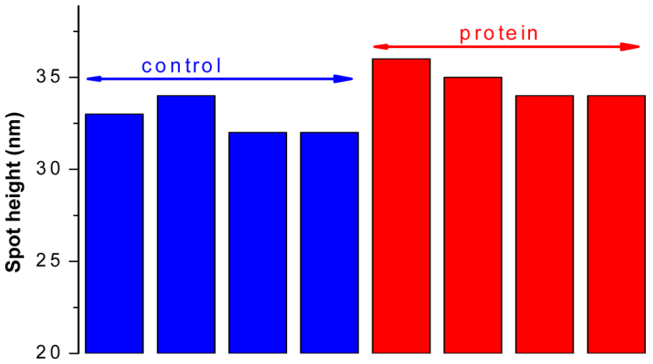

Figure 6. Nanoisland height distribution (four measurements) of samples before (blue bars) and after protein deposition (red bars).

free radicals. Although the possibility of the existence of free radicals on the plasma-treated surfaces cannot be excluded, such radicals are not expected on surfaces for ion implantation voltages less than 400 V,[29] as it is in our case (bias voltage of 100 V). Therefore, the potential of our plasma-treated SiO_2 surfaces to covalently bind biomolecules can be attributed more to the presence of carboxyl or carbonyl groups on the surface than to the presence of free radicals. In addition, no deterioration of the biomolecule immobilization capability of the plasma-treated SiO_2 surfaces was observed with aging, as it would be expected in the case of free radicals.

4. CONCLUSIONS

In this work, a novel, rapid and cost-efficient method for high-density protein nanopatterning appropriate for the modification on large surfaces is demonstrated on Si substrates. The method is based on colloidal lithography combined with plasma-induced surface modification to enable selective protein immobilization on C_4F_8 plasma-treated SiO_2 nanoislands and not on the surrounding Si surface. The thickness of the selectively immobilized protein monolayer on SiO_2 was estimated after height distribution analysis of AFM images before and after protein deposition. Extensive chemical characterization of the surfaces was performed combining XPS analysis and reaction with biomolecules that form covalent bonds with carboxyl or carbonyl groups, to detect the functional groups that are formed on the C_4F_8 plasma-treated surfaces. The confirmed presence of such functional groups on the surface of SiO_2 surfaces, as a result of selective plasma modification of our substrates, suggests the possibility of covalent protein binding on C_4F_8 plasma-modified SiO_2 surfaces apart from physical adsorption. Such fabricated protein nanopatterned substrates can be applied in biosensors for enhanced detection sensitivity, as model substrates for protein–protein interaction studies, as well as substrates for cell cultivation and tissue engineering.

■ ASSOCIATED CONTENT

Ⓢ Supporting Information

High-resolution XPS C_{1S} spectra (and their deconvolution) for untreated and C_4F_8 plasma-treated Si and SiO_2 surfaces. This material is available free of charge via the Internet at http://pubs.acs.org.

■ AUTHOR INFORMATION

Corresponding Author

*Angeliki Tserepi: e-mail, atserepi@imel.demokritos.gr.

Notes

The authors declare no competing financial interest.

■ ACKNOWLEDGMENTS

The authors acknowledge C. Skoulikidou for SEM imaging (Institute of Microelectronics, N.C.S.R "Demokritos") and Dr. S. Pagakis and E. Rigana (Center of Basic Research, Biomedical Research Foundation of Academy of Athens) for confocal microscopy imaging.

■ REFERENCES

(1) Espina, V.; Woodhouse, E. C.; Wulfkuhle, J.; Asmussen, H. D.; Petricoin, E. F.; Liotta, L. A. Protein microarray detection strategies: focus on direct detection technologies. *J. Immunol. Methods* **2004**, *290* (1–2), 121–133.

(2) Michaud, G. A.; Bangham, R.; Salcius, M.; Predki, P. F. Functional protein microarrays for pathway mapping. *Drug Discovery Today: TARGETS* **2004**, *3* (6), 238–245.

(3) Templin, M. F.; Stoll, D.; Schwenk, J. M.; Pötz, O.; Kramer, S.; Joos, T. O. Protein microarrays: Promising tools for proteomic research. *Proteomics* **2003**, *3* (11), 2155–2166.

(4) Aydin, D.; Schwieder, M.; Louban, I.; Knoppe, S.; Ulmer, J.; Haas, T. L.; Walczak, H.; Spatz, J. P. Micro-Nanostructured Protein Arrays: A Tool for Geometrically Controlled Ligand Presentation. *Small* **2009**, *5* (9), 1014–1018.

(5) Hoff, J. D.; Cheng, L.-J.; Meyhöfer, E.; Guo, L. J.; Hunt, A. J. Nanoscale Protein Patterning by Imprint Lithography. *Nano Lett.* **2004**, *4* (5), 853–857.

(6) Keegan, N.; Suarez, G.; Spoors, J. A.; Ortiz, P.; Hedley, J.; McNeil, C. J. A microfabrication compatible approach to 3-dimensional patterning of bio-molecules at Bio-MEMS and biosensor surfaces. Biomedical Circuits and Systems Conference, 2009. BioCAS 2009. IEEE, 26–28 Nov 2009; 2009; pp 17-20.

(7) Lisboa, P.; Valsesia, A.; Colpo, P.; Rossi, F.; Mascini, M. Nanopatterned Surfaces for Bio-Detection. *Anal. Lett.* **2010**, *43* (10), 1556–1571.

(8) Mendes, P.; Yeung, C.; Preece, J. Bio-nanopatterning of Surfaces. *Nanoscale Res. Lett.* **2007**, *2* (8), 373–384.

(9) Malainou, A.; Petrou, P. S.; Kakabakos, S. E.; Gogolides, E.; Tserepi, A. Creating highly dense and uniform protein and DNA microarrays through photolithography and plasma modification of glass substrates. *Biosens. Bioelectron.* **2012**, *34* (1), 273–281.

(10) Zhang, J.; Li, Y.; Zhang, X.; Yang, B. Colloidal Self-Assembly Meets Nanofabrication: From Two-Dimensional Colloidal Crystals to Nanostructure Arrays. *Adv. Mater.* **2010**, *22* (38), 4249–4269.

(11) Taylor, Z. R.; Patel, K.; Spain, T. G.; Keay, J. C.; Jernigen, J. D.; Sanchez, E. S.; Grady, B. P.; Johnson, M. B.; Schmidtke, D. W. Fabrication of Protein Dot Arrays via Particle Lithography. *Langmuir* **2009**, *25* (18), 10932–10938.

(12) Valsesia, A.; Mannelli, I.; Colpo, P.; Bretagnol, F.; Rossi, F. Protein Nanopatterns for Improved Immunodetection Sensitivity. *Anal. Chem.* **2008**, *80* (19), 7336–7340.

(13) Lee, S.-H.; Lee, C.-S.; Shin, D.-S.; Kim, B.-G.; Lee, Y.-S.; Kim, Y.-K. Micro protein patterning using a lift-off process with fluorocarbon thin film. *Sens. Actuators, B* **2004**, *99* (2–3), 623–632.

(14) Pi, F.; Dillard, P.; Limozin, L.; Charrier, A.; Sengupta, K. Nanometric Protein-Patch Arrays on Glass and Polydimethylsiloxane for Cell Adhesion Studies. *Nano Lett.* **2013**, *13* (7), 3372–3378.

(15) Singh, G.; Griesser, H. J.; Bremmell, K.; Kingshott, P. Highly Ordered Nanometer-Scale Chemical and Protein Patterns by Binary Colloidal Crystal Lithography Combined with Plasma Polymerization. *Adv. Funct. Mater.* **2011**, *21* (3), 540–546.

(16) Wood, M. A. Colloidal lithography and current fabrication techniques producing in-plane nanotopography for biological applications. *J. R. Soc. Interface* **2007**, *4* (12), 1–17.

(17) Kristensen, S. H.; Pedersen, G. A.; Ogaki, R.; Bochenkov, V.; Nejsum, L. N.; Sutherland, D. S. Complex protein nanopatterns over

562 large areas via colloidal lithography. *Acta Biomater.* **2013**, *9*, 6158−
563 6168.
564 (18) Singh, G.; Gohri, V.; Pillai, S.; Arpanaei, A.; Foss, M.; Kingshott,
565 P. Large-Area Protein Patterns Generated by Ordered Binary Colloidal
566 Assemblies as Templates. *ACS Nano* **2011**, *5* (5), 3542−3551.
567 (19) Yap, F. L.; Zhang, Y. Protein Micropatterning Using Surfaces
568 Modified by Self-Assembled Polystyrene Microspheres. *Langmuir*
569 **2005**, *21* (12), 5233−5236.
570 (20) Zhang, J.; Yang, B. Patterning Colloidal Crystals and
571 Nanostructure Arrays by Soft Lithography. *Adv. Funct. Mater.* **2010**,
572 *20* (20), 3411−3424.
573 (21) Ogaki, R.; Bennetsen, D. T.; Bald, I.; Foss, M. Dopamine-
574 Assisted Rapid Fabrication of Nanoscale Protein Arrays by Colloidal
575 Lithography. *Langmuir* **2012**, *28* (23), 8594−8599.
576 (22) Choi, D.-G.; Yu, H. K.; Jang, S. G.; Yang, S.-M. Colloidal
577 Lithographic Nanopatterning via Reactive Ion Etching. *J. Am. Chem.*
578 *Soc.* **2004**, *126* (22), 7019−7025.
579 (23) Agheli, H.; Malmström, J.; Larsson, E. M.; Textor, M.;
580 Sutherland, D. S. Large Area Protein Nanopatterning for Biological
581 Applications. *Nano Lett.* **2006**, *6* (6), 1165−1171.
582 (24) Pistillo, B. R.; Gristina, R.; Sardella, E.; Lovascio, S.; Favia, P.;
583 Nardulli, M.; d'Agostino, R. Plasma Processes Combined with
584 Colloidal Lithography to Produce Nanostructured Surfaces for Cell-
585 Adhesion. *Plasma Processes Polym.* **2009**, *6* (S1), S61−S64.
586 (25) Sardella, E.; Lovascio, S.; Favia, P.; d'Agostino, R. Colloidal
587 Monolayers Combined with Cold Plasmas: A Versatile Nano-
588 fabrication Tool. *Plasma Processes Polym.* **2007**, *4* (S1), S887−S890.
589 (26) Valsesia, A.; Colpo, P.; Manso Silvan, M.; Meziani, T.; Ceccone,
590 G.; Rossi, F. Fabrication of Nanostructured Polymeric Surfaces for
591 Biosensing Devices. *Nano Lett.* **2004**, *4* (6), 1047−1050.
592 (27) Denis, F. A.; Hanarp, P.; Sutherland, D. S.; Gold, J.; Mustin, C.;
593 Rouxhet, P. G.; Dufrêne, Y. F. Protein Adsorption on Model Surfaces
594 with Controlled Nanotopography and Chemistry. *Langmuir* **2002**, *18*
595 (3), 819−828.
596 (28) Bayiati, P.; Malainou, A.; Matrozos, E.; Tserepi, A.; Petrou, P. S.;
597 Kakabakos, S. E.; Gogolides, E. High-density protein patterning
598 through selective plasma-induced fluorocarbon deposition on Si
599 substrates. *Biosens. Bioelectron.* **2009**, *24* (10), 2979−2984.
600 (29) Bilek, M. M. M.; Bax, D. V.; Kondyurin, A.; Yin, Y.; Nosworthy,
601 N. J.; Fisher, K.; Waterhouse, A.; Weiss, A. S.; dos Remedios, C. G.;
602 McKenzie, D. R. Free radical functionalization of surfaces to prevent
603 adverse responses to biomedical devices. *Proc. Natl. Acad. Sci. U. S. A.*
604 **2011**, *108* (35), 14405−14410.
605 (30) Wang, C.; Yap, F. L.; Zhang, Y. Micropatterning of polystyrene
606 nanoparticles and its bioapplications. *Colloids Surf., B* **2005**, *46* (4),
607 255−260.
608 (31) Ellinas, K.; Smyrnakis, A.; Malainou, A.; Tserepi, A.; Gogolides,
609 E. Mesh-assisted" colloidal lithography and plasma etching: A route to
610 large-area, uniform, ordered nano-pillar and nanopost fabrication on
611 versatile substrates. *Microelectron. Eng.* **2011**, *88* (8), 2547−2551.
612 (32) Valsesia, A.; Meziani, T.; Bretagnol, F.; Colpo, P.; Ceccone, G.;
613 Rossi, F. Plasma assisted production of chemical nano-patterns by
614 nano-sphere lithography: application to bio-interfaces. *J. Phys. D: Appl.*
615 *Phys.* **2007**, *40* (8), 2341−2347.
616 (33) Jandt, K. D. Atomic force microscopy of biomaterials surfaces
617 and interfaces. *Surf. Sci.* **2001**, *491* (3), 303−332.
618 (34) Tencer, M.; Charbonneau, R.; Lahoud, N.; Berini, P. AFM study
619 of BSA adlayers on Au stripes. *Appl. Surf. Sci.* **2007**, *253* (23), 9209−
620 9214.
621 (35) Lee, M. R.; Fauchet, P. M. Two-dimensional silicon photonic
622 crystal based biosensing platform for protein detection. *Opt. Express*
623 **2007**, *15* (8), 4530−4535.
624 (36) Yin, Y.; Bax, D.; McKenzie, D. R.; Bilek, M. M. M. Protein
625 immobilization capacity and covalent binding coverage of pulsed
626 plasma polymer surfaces. *Appl. Surf. Sci.* **2010**, *256* (16), 4984−4989.